Quantum-chromodynamic predictions for high-p_T baryon production

J. F. Owens
Physics Department, Florida State University, Tallahassee, Florida 32306
(Received 26 December 1978; revised manuscript received 8 March 1979)

Predictions for high-p_T hadron production based on lowest-order quantum-chromodynamic (QCD) perturbation theory are reexamined in the light of new precise data relevant to the determination of the parton fragmentation functions. In particular, predictions for both p and $\bar{p}$ production are given. It is found that for meson production in pp interactions the lowest-order QCD perturbation-theory predictions become dominant in the region $\sqrt{s} > 50$ GeV and $p_T > 5$ GeV/c. On the contrary, for baryon production the lowest-order predictions do not dominate until significantly larger p_T values are reached.

I. INTRODUCTION

Many calculations have now been performed which attempt to describe high-p_T meson production using lowest-order quantum-chromodynamics (QCD) perturbation theory for calculating the hard-scattering subprocesses. The results of these calculations suggest that if the QCD-predicted scaling violations and running coupling constant are retained, then the lowest-order subprocesses can adequately describe the data for sufficiently high energies and large momentum transfers.[1-3] Other analyses have suggested that the range of agreement can be significantly enlarged if one invokes smearing corrections attributed to the transverse motion of the colliding (and fragmenting) partons.[4-7] However, to date, predictions for high-p_T baryon production using the full set of lowest-order subprocesses and including all the predicted scale-violating effects have been absent from the literature. This situation has existed primarily because of the lack of deep-inelastic baryon production data which are necessary in order to determine the parton fragmentation functions for baryons. Recently, however, new data for p and $\bar{p}$ production in both electroproduction and e^+e^- annihilation have become available, thereby making it possible to extend the high-p_T hadron production predictions into the baryon sector.

The applicability of perturbation theory to high-p_T calculations depends crucially on the phenomenon of asymptotic freedom found in QCD.[8,9] Thus, at sufficiently large energies and high p_T it is expected that the lowest-order QCD subprocesses will dominate. However, at low and intermediate p_T higher-order terms should become important. Isolating the effects of these higher-order contributions has historically been rather difficult since attention has been focused, to a large degree, only on single-meson p_T distributions. By varying the species of the produced hadron it should be possible to discern more details of the underlying dynamical mechanisms.

The analysis presented here must, of necessity, simultaneously address both meson and baryon production. The two processes are linked together by the requirement that the parton fragmentation functions satisfy the constraints which follow from momentum conservation. By introducing baryon fragmentation functions, the normalization for the mesonic processes will be decreased somewhat. Considering both processes simultaneously ensures that the successful meson production predictions are retained.

The work reported here took place in two distinct stages. First, it was necessary to determine the parton fragmentation functions for baryons. This necessitated a reanalysis of the fragmentation functions for mesons as well, since the two sets of fragmentation functions are jointly constrained by the requirement of momentum conservation for the fragmenting parton. Having obtained a satisfactory set of fragmentation functions, it was then possible to predict the cross sections for both meson and baryon production at high p_T.

The results obtained here for the meson sector are similar to the results obtained previously in other analyses.[1-7] They are included here both for completeness and in order that one may judge the effect of including baryon production in the analysis of the parton fragmentation functions. These results show that it is possible to describe the leptonic data for both meson and baryon production, and that the resulting predictions for the high-p_T production of mesons are essentially unchanged. Taken together, these two conclusions indicate that the predictions presented here for both proton and antiproton production are indeed representative of the contributions coming from the lowest-order QCD subprocesses.

Section II contains a review of the formalism used in this calculation, including a detailed discussion of the role of parton-transverse-moment-

um smearing. Included, too, are comments on the nature of the higher-order terms which appear in the perturbation-series expansion. In Sec. III the parton fragmentation functions are determined and Sec. IV contains the predictions for high-p_T meson and baryon production. A summary and some conclusions are presented in Sec. V.

II. THEORETICAL PRELIMINARIES

Before addressing the problem of predicting high-p_T baryon production it is, perhaps, worthwhile to reflect on some of the progress that has been made in understanding high-p_T hadron production. There are now sound theoretical reasons[10,11] to believe that at sufficiently large energies and high p_T one can use QCD perturbation theory to describe the hard-scattering subprocesses provided that scale-violating parton distribution[13,14] and fragmentation[15,16] functions together with the strong running coupling constant α_s are used. In particular, at the leading-logarithm level these scale-violating functions are process independent. However, a straightforward application of these ideas results in predictions which fall below the data in the region below $p_T \simeq 5$ GeV/c. Furthermore, when two-particle correlations are studied, significant deviations from the expected planar event structure are observed.[17] For both of these reasons, the original perturbative calculations have been modified to allow for the presence of transverse motion for the colliding and fragmenting partons.[4-7] It is argued[18] that two effects must be taken into account for intermediate p_T values. The first is that the confinement mechanism, operating over a long time scale, gives rise to an intrinsic (or primordial) component of parton transverse momentum. This component is, presumably, characteristic of the colliding hadron and, hence, should not depend on the various kinematic variables, nor should it depend on specific parton flavors. Second, in higher orders of perturbation theory one encounters more complicated subprocesses than the lowest-order $2 \to 2$ type. Specifically, in the next order one finds $2 \to 3$ subprocesses involving, for example, gluon bremsstrahlung as in $qq \to qqg$. Now, to leading-logarithm accuracy, the scale-violating parton distribution and fragmentation functions already account for those contributions which arise from the regions of phase space where the gluon is parallel to one of the quarks.[20] However, the contributions where the gluon and quarks are all distinct, i.e., three-high-p_T-jet final states, are not included. These terms can give contributions to the single-particle spectra and, in particular, should modify the predicted planar event structure.

The calculation in Ref. 6 utilized a moderate estimate for the average value of the parton transverse momentum $\langle k_T \rangle$, which was intended to represent only the intrinsic component. This resulted in an extension of the region of agreement with the data. This region was increased further in Refs. 4, 5, and 7, where larger values of $\langle k_T \rangle$ were employed in an attempt to account for the effects of the higher-order terms in a phenomenological fashion. In this manner the data can be described successfully over the range $p_T \gtrsim 2$ GeV/c for center-of-mass energies $\sqrt{s}$ above 20 GeV. This phenomenological type of smearing calculation has recently been criticized, however, on the basis that if off-shell kinematics is used for the colliding partons, then the smearing effects become greatly reduced.[21]

It has been argued[22] that in place of large smearing corrections, one should instead include effects from other higher-order diagrams involving, for example, initial states with more than two partons, e.g., $(q\bar{q})\, q \to (q\bar{q})q$. Such terms arise in the constituent-interchange model (CIM) and correspond, in this case, to meson-quark elastic scattering. When interpreted in this manner the CIM appears as an integral part of the complete QCD theory. Thus, a complete calculation should involve the scattering of all the possible components of the incoming hadronic wave functions.

It has thus far been difficult to discount completely either the CIM approach or that which invokes large smearing corrections. This is likely to be due to the fact that there is an element of truth in both types of calculations. To see this, consider the three types of tests which have been most extensively studied. The simplest observable is the p_T distribution at fixed energy. Here both types of calculations can achieve agreement with the data. It is possible to go further by studying the p_T dependence at fixed x_T and θ. In a scale-invariant model the invariant cross section is expected to behave as

$$E d^3\sigma/dp^3 = A p_T^{-n} f(x_T, \theta) . \tag{1}$$

For the CIM $n = 8$,[23] while for the simplest QCD subprocesses $n = 4$. However, inclusion of all the predicted scaling violations and the use of the strong running coupling constant yields $n \simeq 6.5$.[3-7] Including large k_T smearing effects can raise this value to $n \simeq 8$ over a limited kinematic range. Therefore, consideration of the meson data alone, for which $n \simeq 8$, is not sufficient to discriminate between the two approaches. Finally, studies of two-particle correlation data show that the lowest-order QCD subprocesses together with substantial k_T smearing can account for the observed effects.[5] Here, too, proponents of the CIM claim to be able

to understand the data, although quantitative calculations thus far are lacking.

From the above discussion it is clear that one of the problems in discriminating between the two types of calculations is due to the fact that their predictions are rather similar for meson production. The CIM scaling behavior ($n = 8$) is not radically different from that predicted by QCD ($n \simeq 6.5$ in the currently accessible kinematic region). The difference is small enough to be accounted for by parton k_T effects. Consider, however, the corresponding predictions for baryon production. Here the relevant CIM diagrams predict $n = 12$ while the predictions of the lowest-order QCD subprocesses remain essentially unchanged. It is therefore possible that clearer distinction between the two types of calculations can be obtained by studying high-p_T baryon production.[24]

The basic idea that will be pursued here is to make use of the predictive power of perturbative QCD calculations. To this end, only the lowest-order $2 \to 2$ subprocesses will be considered at this time. The expressions for the relevant cross sections are well known and can be found, for example, in Refs. 1–3. Once the input functions have been determined using deep-inelastic scattering data, the remaining large degrees of freedom are associated with the treatment of the parton k_T smearing and, to some extent, the choice of the input gluon distribution function. In an effort to retain the strong predictive power of the perturbative approach, only the effects of the intrinsic parton k_T will be included in this calculation. Thus, the effects of the higher-order terms, accounted for previously in a phenomenological manner by using a large value for $\langle k_T \rangle$, will not be included here. Typical uncertainties associated with the gluon distribution will be assessed by using two representative forms. Each of these points will now be discussed in detail.

In order to treat the question of the parton k_T smearing properly, it is necessary to find a method of estimating the amount of intrinsic transverse momentum which can be associated with the various hadronic wave functions. One source of such information is provided by the hadronic production of dileptons. A naive interpretation of the basic Drell-Yan[25] mechanism for dilepton production would suggest that the observed dilepton transverse-momentum distribution results from a convolution of colliding quark and antiquark k_T distributions. However, a study of QCD perturbation theory reveals contributions arising from the processes $q\bar{q} \to \mu^+ \mu^- g$ and $qg \to q\mu^+ \mu^-$.[26–28] In fact, in QCD it is only after integration over the dilepton transverse momentum that one recovers the usual Drell-Yan formula, only now with scale-violating parton distribution functions.[31] Now it is possible to investigate the nature of the intrinsic k_T distribution by first calculating the perturbative contribution to $\langle p_T^2 \rangle$ for the dileptons, and subtracting this from the observed value. This procedure has been followed using dimuon data[32] at 400 GeV/c. The observed value for $\langle p_T^2 \rangle$ lies about 1.1 (GeV/c)^2 above the perturbative contribution.[33] This excess is then defined as being the contribution from the intrinsic parton transverse momentum. Assuming a Gaussian form for this distribution yields $\langle k_T^2 \rangle = 0.55$ (GeV/c)^2 and $\langle k_T \rangle = 660$ MeV/c. Similar values have been obtained using alternate prescriptions.[19,26] It should be stressed that this method defines the intrinsic component of the k_T distribution in terms of the perturbation-series expansion. If effects from yet higher-order terms were included then the value of $\langle k_T^2 \rangle$ would be somewhat decreased. It should also be pointed out that if nuclear target effects are creating anomalously large values of $\langle p_T^2 \rangle$ for the dimuon pairs, then the actual value for the intrinsic portion of the k_T distribution could be smaller than that obtained here.[34] Nevertheless, arguments have been given which show that $\langle k_T \rangle \sim 600$ MeV/c is not an unreasonable value for the intrinsic contribution.[30]

The k_T smearing for the high-p_T hadron production calculations has been performed using the above value for $\langle k_T \rangle$. Thus, only the intrinsic contribution is included and the overall smearing is less than in other calculations.[4,5,7] For the transverse momentum associated with the final-state fragmentation process a Gaussian distribution with $\langle k_T \rangle = 440$ MeV/c has been used, as suggested by the analysis of quark fragmentation given in Ref. 35. Note that since only the intrinsic contribution to the various k_T distributions is being included here, no distinction is being made between the quark and gluon values for $\langle k_T \rangle$ in either the distribution or fragmentation functions. This is reasonable for that transverse motion due to confinement, although some differences should arise in the effective k_T distributions if higher-order terms are included.[7]

With the reduced value of $\langle k_T \rangle$ used here the results are insensitive to the use of off-shell kinematics for the partons. Furthermore, there is no need to employ model-dependent mass parameters or cutoffs. The k_T smearing employed here gives rise to only a modest increase in the cross section, e.g., slightly less than a factor of 2 at $\sqrt{s} = 62.4$ GeV and $p_T = 3$ GeV/c.

In any test of a theory which relies on absolute normalization it is necessary to assess the various sources of uncertainty which may enter. In

this analysis the most precise leptonic data available have been used to determine the input fragmentation and distribution functions and there is very little freedom for alteration in them. However, there is a major source of ambiguity related to the choice of the gluon distribution function. The input quark distributions used here are the same as were used in Ref. 7. For the gluon distributions, however, two choices will be used. The first is proportional to the one used in Refs. 4 and 5,

$$xG(x,Q_0^2)=0.892(1+9x)(1-x)^4. \tag{2}$$

The normalization has been fixed by utilizing the constraint of momentum conservation in conjunction with the input quark distributions. The second form is that used in Ref. 7,

$$xG(x,Q_0^2)=2.676(1-x)^5\ . \tag{3}$$

In each instance, the distribution functions for $Q^2>Q_0^2$ were determined using the appropriate Mellin transform techniques. As in the previous analysis[7] $Q_0^2=4$ (GeV/c)^2 has been used. The strong running coupling constant has been taken as $\alpha_s=12\pi/[25\ln(Q^2/\Lambda^2)]$, corresponding to four quark flavors. For the scale parameter Λ the value $\Lambda=400$ MeV/c has been chosen. The same Q^2 definition[4] has been used as before,

$$Q^2=2stu/(s^2+t^2+u^2), \tag{4}$$

where s, t, and u are the Mandelstam variables for the parton-parton scattering subprocess. The use of two sets of gluon distributions gives an estimate of the effect of the single largest source of ambiguity in this analysis. Additional normalization uncertainties associated with the fragmentation functions will be discussed in the following section.

In summary, this analysis is intended to be an accurate representation of the predictions of the lowest-order QCD $2\to 2$ subprocesses. Only the parton-transverse-momentum smearing associated with the intrinsic contribution is included. It is therefore expected that the (incomplete) theoretical predictions will lie below the data in the intermediate-p_T region. The difference between these predictions and the data will thus provide a bound on the contributions of the remaining higher-order terms such as multijet final states, CIM diagrams, etc. The variation of this bound with produced particle species should provide useful information as to the nature of these additional contributions.

III. PARTON FRAGMENTATION FUNCTIONS

In Ref. 3 a set of parton fragmentation functions for mesons was presented. These functions were constrained by various sum rules and by (broken) SU(3) symmetry considerations. They were shown to give a good representation of the data. For quark fragmentation these functions were based on a simple picture wherein a valence-sea decomposition was used. The valence term corresponds to the situation where the initial quark ends up in the observed meson. The sea term then describes the case where a quark-antiquark pair is created during the fragmentation process and the observed meson does not contain the initial quark.

New data involving, in particular, $K^{\pm}$ electroproduction[36] have shown that this simple picture is incomplete and that effects due to resonance decays must also be included.[35,37,38] Therefore, this model has been updated to include these effects. The technique used to handle the resonance decays is the same as that presented in Ref. 35. Simple two-body decay kinematics is used together with the parent-child relation to determine the resulting longitudinal-momentum distribution of the decay products. For decays involving more than two mesons, the results are weighted so as to produce the correct decay multiplicity.[35] This approximation procedure correctly describes the dominant decay modes and is adequate for the more complicated, though less important, high-multiplicity final states. The quark distributions for the parent (or primary) mesons are parametrized in the valence-sea fashion as in Ref. 3. In this case, however, both pseudoscalar and vector mesons are produced with relative probabilities α_P and α_V. Following Ref. 35, $\alpha_P=\alpha_V=0.5$ has been used. It is then straightforward to write down the independent primary fragmentation functions for the quarks. These are

$$\begin{aligned}
zD_{\pi^+/u}(z,Q_0^2)&=a\sqrt{z}\,(c-z)+\xi_\pi(1-z)^2,\\
zD_{\pi^-/u}(z,Q_0^2)&=\xi_\pi(1-z)^2,\\
zD_{K^+/u}(z,Q_0^2)&=b\sqrt{z}\,(c-z)+\xi_\pi(1-z)^2,\\
zD_{K^-/u}(z,Q_0^2)&=\xi_K(1-z)^2,\\
zD_{K^-/s}(z,Q_0^2)&=a\sqrt{z}\,(c-z)+\xi_K(1-z)^2,
\end{aligned} \tag{5}$$

where z is the longitudinal-momentum fraction of the observed meson. Similar expressions hold for the production of vector mesons. The other π and K (ρ and K^*) functions may be obtained via the relations found in Ref. 3. However, in order to determine the η and η' (ω and ϕ) functions, the relevant mixing angles must be specified. For the vector-meson case, $\theta_V=\tan^{-1}1/\sqrt{2}$ was chosen so that the quark content of the ϕ is pure $s\bar{s}$. For the pseudoscalar mixing angle, a value of $\theta_P=-9.7^\circ$ was chosen so that both the η and η' have equal quantities of strange and nonstrange quarks.[35]

The resulting fragmentation functions are (the z and Q^2 dependences have been suppressed for compactness)

$$
\begin{aligned}
&zD_{\omega/u}=zD_{\rho^0/q},\quad zD_{\omega/\bar{q}}=zD_{\rho^0/\bar{q}},\\
&zD_{\phi/s}=zD_{\phi/\bar{s}}=R_{K\pi}a\sqrt{z}\,(c-z)+R_{K\pi}{}^2\xi_\pi(1-z)^2,\\
&zD_{\phi/u}=zD_{\phi/\bar{u}}=zD_{\phi/d}=zD_{\phi/\bar{d}}=R_{K\pi}{}^2\xi_\pi(1-z)^2,\\
&zD_{\eta/u}=zD_{\eta/\bar{u}}=zD_{\eta/d}=zD_{\eta/\bar{d}}\\
&\quad=\tfrac{1}{4}a\sqrt{z}\,(c-z)+\tfrac{1}{2}\xi_\pi(1+R_{K\pi}{}^2)(1-z)^2,\\
&zD_{\eta/s}=zD_{\eta/\bar{s}}=\tfrac{1}{2}R_{K\pi}a\sqrt{z}\,(c-z)+\tfrac{1}{2}\xi_\pi(1+R_{K\pi}{}^2)\\
&\qquad\times(1-z)^2,
\end{aligned}
\tag{6}
$$

where $R_{K\pi}\equiv\xi_K/\xi_\pi$ is an SU(3)-breaking factor which takes into account the relative difficulty of creating an s quark versus a u or d quark. With the above choice for the mixing angle θ_P, the η and η' fragmentation functions have the same form. The above expressions completely determine the distributions for the primary mesons. Adding in the decay-product distributions for the primary vector mesons completes the description of the quark fragmentation functions for mesons.

For fragmentation of quarks into baryons the situation is considerably simplified by the observation that in the case of baryon decays the daughter baryons carry most of the parent baryon momentum as a result of the small mass of the daughter pion. Therefore, to a good approximation, one can simply parametrize the final p, $\bar{p}$, n, and $\bar{n}$ decay functions without having to take into account explicitly any intermediate baryon states.[38] These final baryon functions are in fact the relevant ones for most experiments since no distinction is normally made, for example, between direct protons and hyperon-decay products. Furthermore, modifications to the meson distributions due to baryon-decay products should be unimportant since they will dominantly occur at low z values which are unimportant for the applications to be considered here. The parametrization employed here is based on a simple extension of the valence-sea decomposition

$$
\begin{aligned}
&zD_{p/q}=zD_{n/q}=zD_{\bar{p}/\bar{q}}=zD_{\bar{n}/\bar{q}}\\
&\quad=a_p\sqrt{z}\,(1-z)^2+\xi_p(1-z)^3,\\
&zD_{p/\bar{q}}=zD_{n/\bar{q}}=zD_{\bar{p}/q}=zD_{\bar{n}/q}=\xi_p(1-z)^3,
\end{aligned}
\tag{7}
$$

where $q=u$, d, or s. Notice that here the strange quarks enter into the valence expressions. This follows from the fact that there are contributions from hyperon decays for which the strange quarks appear in the valence terms.

The meson and baryon parametrizations for the quark fragmentation functions will be completely determined once the parameters a, b, c, ξ_π, ξ_K, a_p, ξ_p, and P are specified. The last parameter, P, determines the probability of obtaining a meson (as opposed to a baryon) from a quark jet. Several of these parameters can now be constrained by various sum rules.[3,39] First, $R_{K\pi}$ is taken to be 0.5 as in Ref. 3. This is equivalent to the SU(3)-breaking factor used in Ref. 35, as well. For the meson sector the isospin[40] and momentum sum rules yield the contraints

$$
\begin{aligned}
&b=a/2,\quad a(2c-2/3)=\tfrac{2}{5},\\
&\xi_\pi=12/25(1-5ac/3+a).
\end{aligned}
\tag{8}
$$

In addition, the momentum sum rule for the baryon sector yields

$$
\xi_p=1-32a_p/105. \tag{9}
$$

Therefore, the three parameters c, a_p, and P will completely determine the quark fragmentation functions for mesons and baryons. Note, now, that overall momentum conservation requires that the meson functions be multiplied by P and the baryon functions by $1-P$.

Finally, a parametrization for the gluon fragmentation functions must be specified. The forms chosen are

$$
\begin{aligned}
&zD_{\pi/g}=g_\pi(1-z)^{1.5},\quad zD_{K/g}=g_K(1-z)^{1.5},\\
&zD_{\eta/g}=zD_{\eta'/g}=g_\eta(1-z)^{1.5},\\
&zD_{p/g}=zD_{n/g}=zD_{\bar{p}/g}=zD_{\bar{n}/g}=g_N(1-z)^{2.5}.
\end{aligned}
\tag{10}
$$

In each case the power was chosen to be intermediate between the respective valence and sea

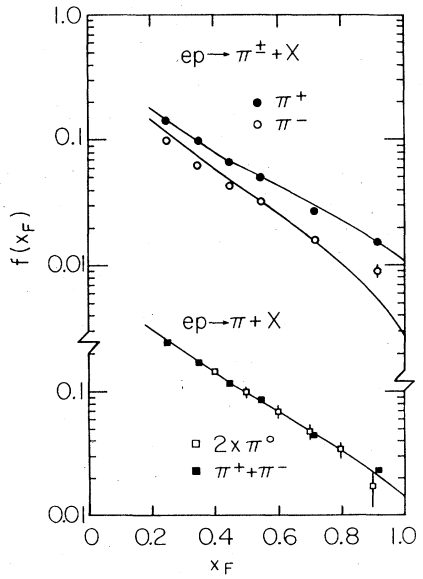

FIG. 1. Result of fitting the fragmentation functions to data for π^+ and π^- (Ref. 36) as well as π^0 (Ref. 41) electroproduction.

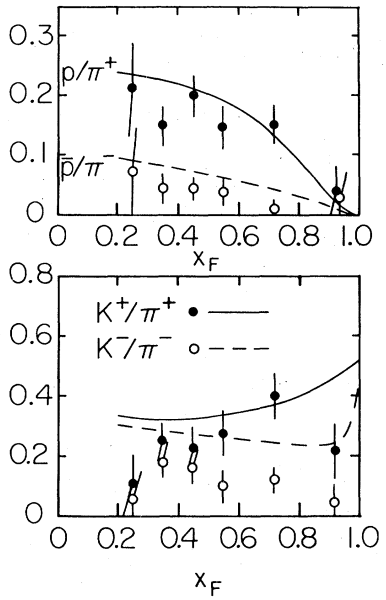

FIG. 2. Fitted results for p, $\bar{p}$, K^+, and K^- electroproduction. The data are from Ref. 36.

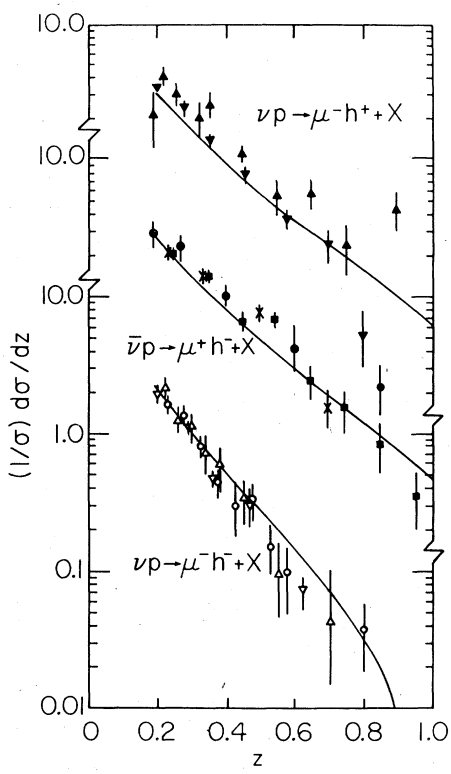

FIG. 3. Predictions for deep-inelastic neutrino and antineutrino reactions. The data are from Ref. 42 (●, ○), Ref. 43 (■), Ref. 44 (▲, △), Ref. 45 (▼, ▽), and Ref. 46 (×).

powers. The various meson coefficients are assumed to be related by the same SU(3) suppression factors observed in the quark-sea terms. Thus, $g_K = R_{K\pi} g_\pi$ and $g_\eta = \frac{1}{2}(1 + R_{K\pi}^2) g_\pi$. It is assumed that the mesons carry a total fraction P of the gluon momentum while baryons carry $1 - P$. The momentum sum rules then yield

$$g_N = 0.875(1 - P) ,$$

$$g_\pi = 0.4P .$$

The remaining parameters (c, a_p, and P) have been determined by fitting data from a SLAC-MIT electroproduction experiment.[36] Note that the variable $x_F = p_l / p_{l\,\max}$ has been used, where p_l is the hadron longitudinal momentum. The results are

$$c = 1.703, \quad a_p = 2.106, \quad P = 0.923 .$$

Equations (8) and (9) then yield

$$a = 0.146, \quad \xi_\pi = 0.351, \quad \xi_p = 0.358 .$$

Notice that only about 8% of the time does a quark fragment into a baryon. Therefore, the meson sector is largely unaffected by the inclusion of the baryon terms.

In Fig. 1 the fitted results are compared with data for $\pi^\pm$ (Ref. 36) and π^0 (Ref. 41) electroproduction. The data are presented in terms of

$$f(x_F) = \frac{1}{2\pi} \frac{2}{\sigma_{\text{tot}}} \int \frac{E}{p_{l\,\max}} \frac{d\sigma}{dx_F dp_T^2 d\phi} dp_T^2 d\phi .$$

The π^- curve falls somewhat more steeply than the data, but the π^+ and π^0 comparisons are excellent. These data have been taken in the kinematic region $0.5 < Q^2 < 7.0$ (GeV/c)^2 and $15 < s < 31$ GeV^2, which corresponds to $0.02 < x < 0.33$ where Q^2, s, and x are the usual electroproduction kinematic variables.[36] The reduced x range enhances slightly the role of the sea quarks. This effect tends to flatten the π^- curve somewhat, though not quite enough. Figure 2 contains the results for the p/π^+, $\bar{p}/\pi^-$, K^+/π^+, and K^-/π^- ratios. More $K^\pm$ production is predicted than is apparent in the data. However, the inclusion of resonance decay effects has resulted in a significant decrease, especially for low values of x_F. The fitted levels of baryon production are in good agreement with the available data. Note, however, that the data do not really determine the $\bar{p}$ production level very accurately in the high-x_F region, and in the low-x_F region there may be a slight tendency to overestimate the data.

In order to serve as a consistency check, the fitted fragmentation functions have been used to predict the results for various neutrino-induced

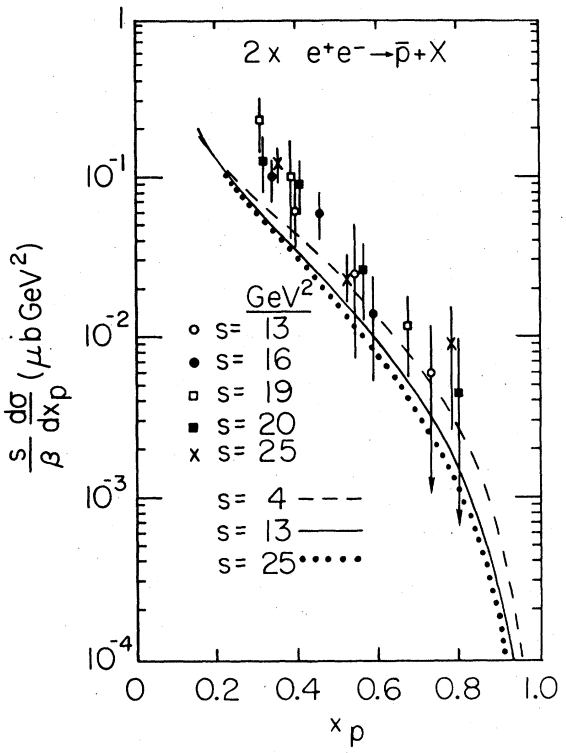

FIG. 4. Predictions for $e^+e^- \to p+\bar{p}+X$. The data are from Ref. 47 and correspond to twice the $\bar{p}$ production cross section. The theoretical predictions are shown for several energies in order to illustrate the magnitude of the scaling violations.

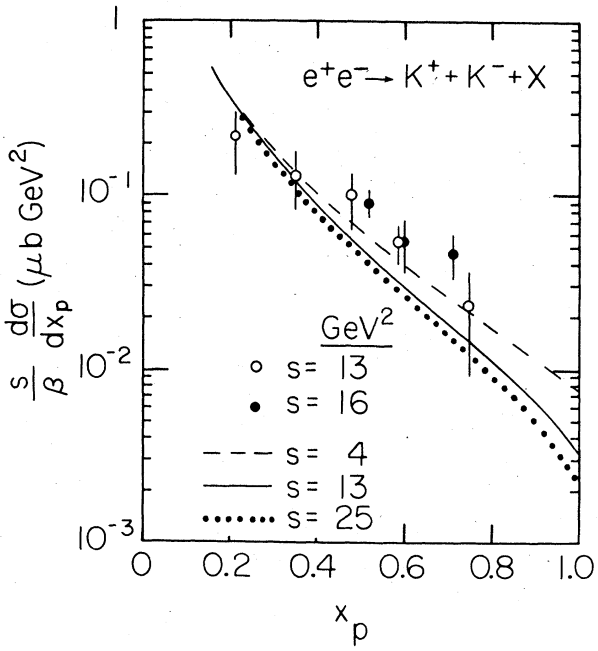

FIG. 5. Same as Fig. 4 except for K^+ and K^- production.

and e^+e^- annihilation experiments. In Fig. 3 the predictions for a variety of neutrino and antineutrino reactions[42-46] are shown. In each case the agreement is good. In Fig. 4 the predictions for $e^+e^- \to (p+\bar{p})+X$ are shown together with data from DESY.[47] The data span a range of energies, so several curves are shown corresponding to $4 \leq s \leq 25$ GeV^2. These results show that the scale-violating effects are rather mild and, further, that the curves underestimate the data. Note that the scaling variable used here is $x_p = 2p/\sqrt{s}$ rather than $x_E = 2E/\sqrt{s}$, which was used originally.[47] The corresponding predictions for $K^\pm$ production are shown in Fig. 5. Here, too, the curves show a tendency to underestimate the data.[47] Thus, for both the $\bar{p}$ and $K^\pm$ cases the fitted results obtained from the electroproduction data are somewhat high while the e^+e^- predictions turn out to be slightly low. In the context of the parton model it is not possible to account for the remaining discrepancies. If they are a result of residual phase-space effects, then data at higher Q^2 and $\sqrt{s}$ will be of some assistance. On the other hand, the e^+e^- data in the region above $\sqrt{s} \simeq 3.7$ GeV may be receiving some contributions from charm decay. These effects are not included in the model.

The present parametrization strikes a balance between the electroproduction[36] and e^+e^- annihilation[47] data and, in so doing, should provide a realistic estimate of the various fragmentation functions. The good agreement found for the neutrino data suggests that this is indeed the case.

IV. HIGH-p_T PREDICTIONS

Predictions for both meson and baryon production at high p_T have been made using as input the parton distribution and fragmentation functions discussed previously. Unless otherwise specified, all the curves presented here have been calculated using the gluon form shown in Eq. (2). The results for pion production are compared with the data[48,49] in Figs. 6 and 7. The predictions are significantly below the data for values of $\sqrt{s}$ between 20 and 30 GeV, with the discrepancy becoming less as p_T is increased. In the upper energy range shown the curves underestimate the data by a factor of about 3 at $p_T = 3$ GeV/c and by $p_T \simeq 5$ GeV/c the curves have intersected the data. This behavior is characteristic of calculations which use little or no parton-k_T smearing and is obtained here since only the intrinsic k_T component is retained. It appears that for $\sqrt{s} \geq 50$ GeV, lowest-order $2 \to 2$ subprocesses account for at least 50% of

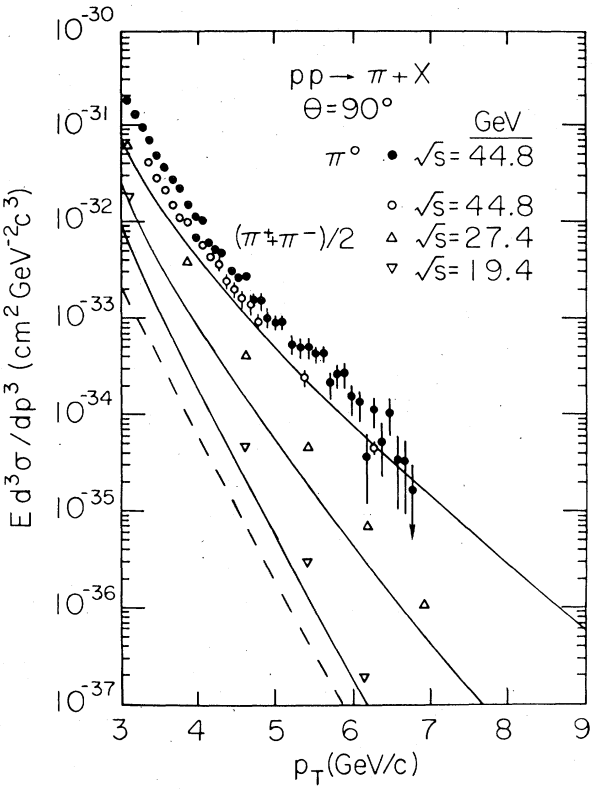

FIG. 6. Predictions for high-p_T pion production. The data are from Ref. 48 (∇, Δ) and Ref. 49 (●, ○). The dashed curve has had the parton-k_T smearing removed and corresponds to $\sqrt{s} = 19.4$ GeV.

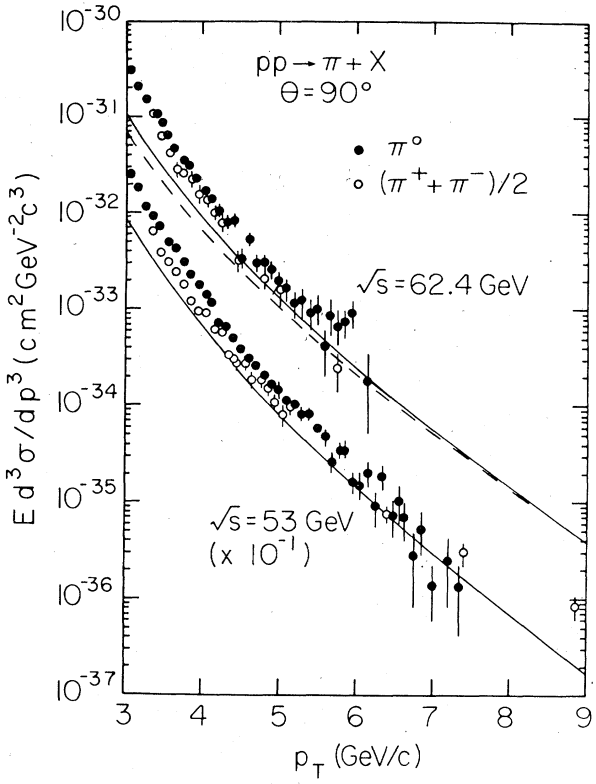

FIG. 7. Predictions for high-p_T pion production. The data are from Ref. 49. The dashed curve has had the parton-k_T smearing removed and corresponds to $\sqrt{s} = 62.4$ GeV. For clarity, both the theoretical curve and the data at $\sqrt{s} = 53$ GeV have been reduced by a factor of 10.

the observed cross section by $p_T \simeq 5$ GeV/c and become dominant for p_T values above this point. In order to check this, precise data at larger p_T values are required. In Fig. 8 predictions are given at two values of $\sqrt{s}$ for $p_T \leq 16$ GeV/c. The upper (lower) curve in each band has been calculated using the gluon distribution given in Eq. (2) [Eq. (3)]. These bands thus show the typical uncertainties associated with the poorly determined gluon distribution. Some data are available in this higher p_T range, but, unfortunately, the different measurements are not in agreement with each other. Preliminary data[50] from an Athens-Brookhaven-CERN-Syracuse-Yale (ABCSY) experiment agree well with the predictions shown in Fig. 8 in the region above $p_T = 5$ GeV/c. It should be noted that these data agree precisely with data[49] in the region below 5 GeV/c, thereby lending credence to their normalization. Data[51] from a CERN-Saclay-Zurich experiment, however, generally lie between a factor of 2–3 higher than the ABCSY data in the region $p_T > 6$ GeV/c. Finally, preliminary data[52] from a CERN-Columbia-Oxford-Rockefeller collaboration lie between the two

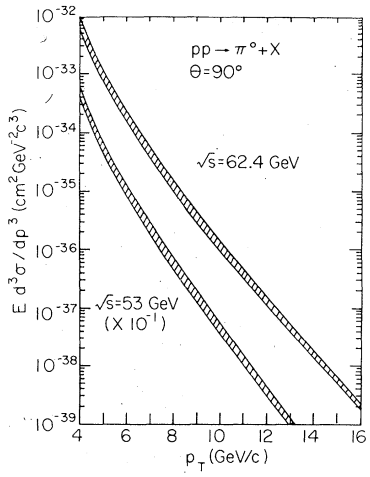

FIG. 8. Predictions for high-p_T π^0 production for two values of $\sqrt{s}$. The shaded bands indicate typical uncertainties associated with the gluon distribution. In each case the upper (lower) curve of the band corresponds to the input gluon expression in Eq. (2) [Eq. (3)]. For clarity, the results for $\sqrt{s} = 53$ GeV have been reduced by a factor of 10.

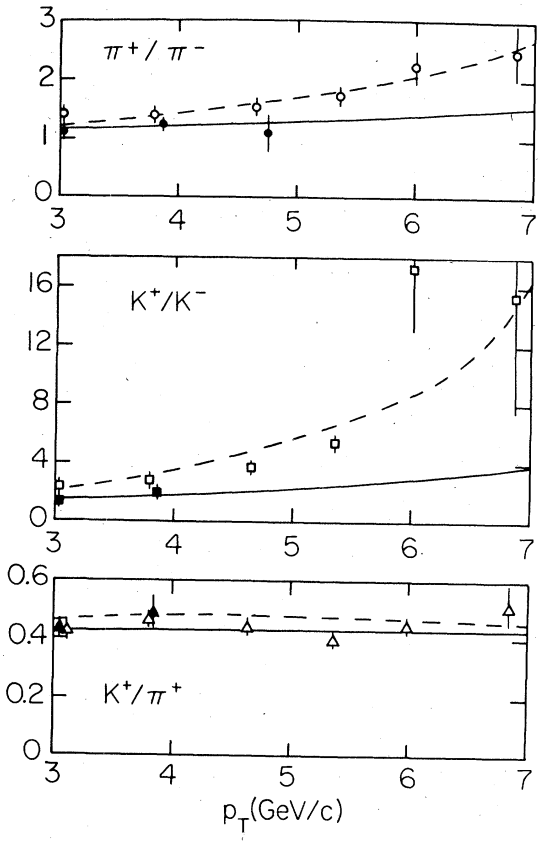

FIG. 9. Predictions for various particle ratios at $\sqrt{s}=27.4$ GeV [dashed curves and open symbols (Ref. 53)] and $\sqrt{s}=53$ GeV [solid curves and closed symbols (Ref. 54)].

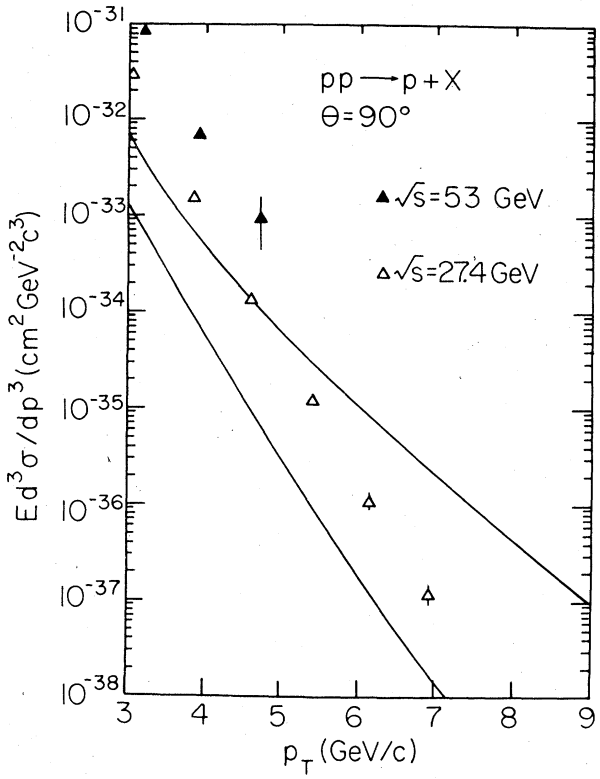

FIG. 10. Predictions for high-p_T proton production. The data are from Ref. 53 (△) and Ref. 54 (▲).

other results with a tendency to be closer to the ABCSY results. Thus, the situation is somewhat unclear at the moment. However, the trend of the available data shows that there is reasonable agreement between the theory and the data in this larger p_T region.

Figure 9 shows the predictions for the π^+/π^-, K^+/K^-, and K^+/π^+ particle ratios at $\sqrt{s}=27.4$ (Ref. 53) and 53 GeV.[54] In each case the predicted magnitudes and energy dependences are in agreement with the data. Therefore, the conclusions reached above for the π^0 data also apply to the production of other pseudoscalar mesons. Notice, too, that the inclusion of resonance effects results in a K^+/π^+ ratio of nearly $\frac{1}{2}$ for high-p_T meson production in agreement with the data, while also yielding a much smaller ratio for the region of x_F covered by the electroproduction data. This point has been stressed in Ref. 37.

Figures 10 and 11 show the predictions for high-p_T p and $\bar{p}$ production at $\sqrt{s}=27.4$ and 53 GeV. It is clear that the discrepancy between the theoretical predictions and the data[53,54] is significantly greater than was the case for the meson sector. At $p_T=3$ GeV/c the data exceed the theoretical curves by factors of 25 and 15 at $\sqrt{s}=27.4$ and 53 GeV, respectively, for proton production. For $\bar{p}$ production the corresponding factors are 8 and 13.[55] These figures are to be compared with those for the meson case which are 3.3 and 3 at $p_T=3$ GeV/c and $\sqrt{s}=27.4$ and 53 GeV, respectively. It is clear, then, that the lowest-order predictions at $p_T=3$ GeV/c lie increasingly below the data as one goes from meson to $\bar{p}$ to p production. Data for p and $\bar{p}$ production do not exist in the region $\sqrt{s}>50$ GeV and $p_T>5$ GeV/c, where the lowest-order predictions for meson production begin to dominate. However, Figs. 10 and 11 show that there appears to be a convergence of the theory towards the data as p_T is increased. This behavior is expected, of course, and it is anticipated that at sufficiently large p_T and s values the lowest-order predictions will become dominant, just as in the meson sector.

At this point it is reasonable to ask: What factors exist which could affect the normalization of the baryon predictions in the context of lowest-

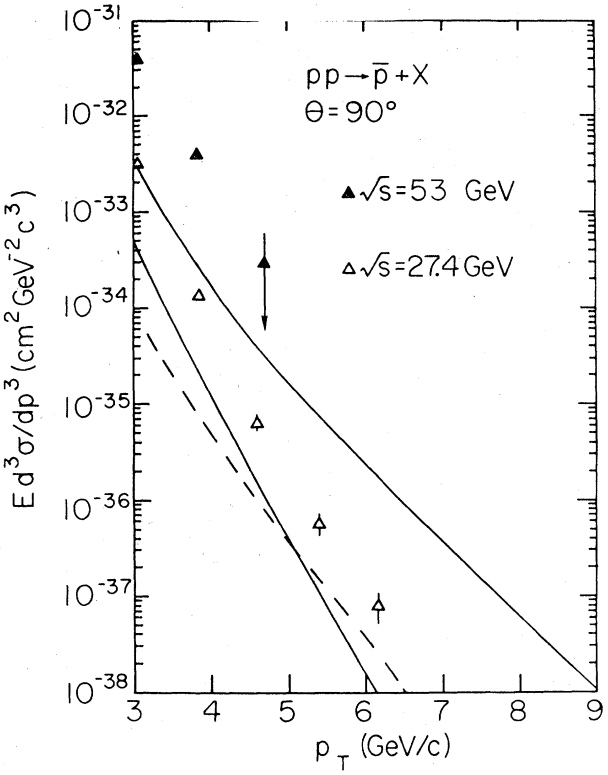

FIG. 11. Predictions for high-p_T antiproton production. The data are from Ref. 53 (△) and Ref. 54 (▲). The dashed curve is a theoretical prediction from Ref. 24 corresponding to a lowest-order QCD calculation with exact scaling.

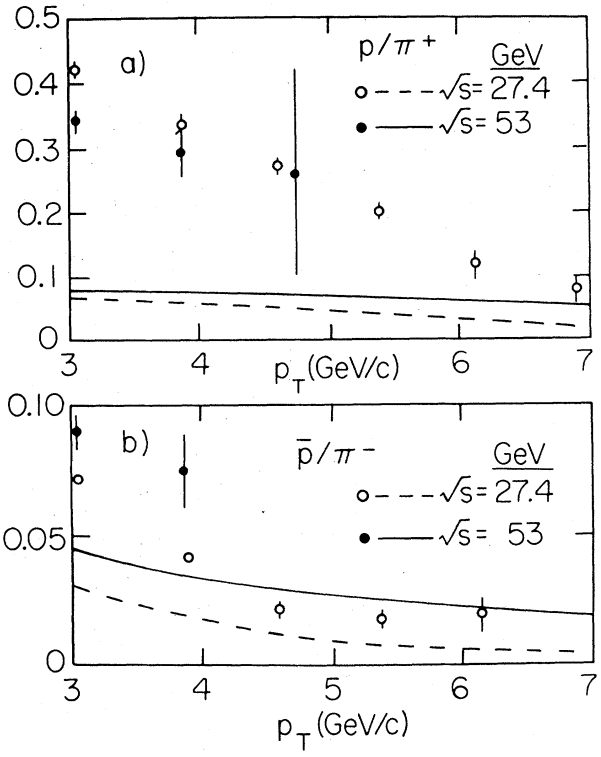

FIG. 12. Predictions for high-p_T p/π^+ and $\bar{p}/\pi^-$ ratios at $\sqrt{s}=27.4$ GeV [dashed curves and open symbols (Ref. 53)] and $\sqrt{s}=53$ GeV [solid curves and closed symbols (Ref. 54)].

order QCD perturbation theory? One such factor is the larger mass of the produced baryons compared to the meson masses. In this calculation the external masses have been retained so that the kinematic variables have the correct mass dependences. External masses also enter into the definitions of the scaling variables used in determining the fragmentation functions. For example, the electroproduction data used here[36] are given in terms of x_F while the e^+e^- annihilation data[47] are given in terms of x_E. In order to facilitate comparison between the two data sets, the e^+e^- data have been displayed in terms of x_p, as mentioned above in Sec. III. Although all three variables are equivalent in the high-energy limit, at the energies of the present experiments x_p more closely approximates x_F than does x_E. This change of variables shifts the e^+e^- data to lower x_p values since $x_p<x_E$. Also, the data are lowered by the amount p/E. This variable transformation has the effect of bringing the theoretical predictions, obtained by fitting the electroproduction data, into better agreement with the e^+e^- data. The slight underestimates apparent in Figs. 4 and 5 would have been much larger had the variable x_E been retained. The results shown in Figs. 2, 4, and 5 indicate that the present parametrization gives a compromise between the electroproduction and e^+e^- data. It seems unlikely that an alternate choice of scaling variables could retain the agreement with the leptonic data while simultaneously increasing the high-p_T predictions. In this regard, it should be stressed that the $K^\pm$ predictions are also affected by this same uncertainty, although to a lesser extent, and they are in good agreement with the high-p_T data, as is shown in Fig. 9.

Another source of uncertainty concerns gluon-related effects. The relative normalization between meson and baryon fragmentation from a gluon is determined by the probability that a quark jet produces a baryon, as discussed in Sec. III. While this is an assumption, it should provide at least a reasonable estimate for the level of baryon fragmentation from a gluon. At any rate, the single-particle cross section results mainly from quark fragmentation, as a result of the flatter z dependence for the quark frag-

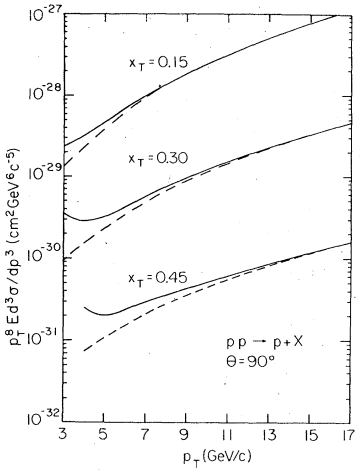

FIG. 13. Predictions for the invariant cross section at 90° for proton production weighted by p_T^8. The dashed lines show the results with the parton-k_T smearing removed.

mentation functions. Therefore, minor variations in the gluon fragmentation functions will not significantly increase the level of the baryon production predictions.

The uncertainty in the gluon distribution functions also affects the baryon-production normalization. This uncertainty is also present for the meson predictions as well, and, therefore, will largely cancel in the ratios p/π^+ and $\bar{p}/\pi^-$. These ratios are shown in Fig. 12 for $\sqrt{s} = 27.4$ and 53 GeV. As noted before, the proton data lie up to an order of magnitude above the predictions, and the antiproton data exceed the predictions by a factor which varies between 2 and 3. While this is comparable to the underestimate observed in Fig. 4 for e^+e^- annihilation, it should be stressed that the same parametrization yields results which are slightly above the electroproduction data shown in Fig. 2. Therefore, unless new electroproduction data indicate a larger degree of antiproton production than is now observed, it would be difficult to significantly increase the predictions shown in Figs. 11 and 12.

Results similar to those presented here have recently been obtained by Gunion and Jones,[24] who studied the transition from the low-p_T region to the region where the lowest-order $2 \rightarrow 2$ subprocesses dominate. For comparison, their lowest-order prediction for $\bar{p}$ production at $\sqrt{s} = 27.4$ GeV is shown in Fig. 11. Their prediction is somewhat flatter than that presented here, primarily due to their assumption of complete scale invariance. Thus, although the calculations differ in detail, the order of magnitude for the lowest-order predictions is the same.

At this point it is necessary to seek an understanding of why the baryon predictions lie much further below the data than do the meson predictions. To understand this behavior one must first understand the effects on the single-particle spectra of the phenomenon of trigger bias. Owing to the steeply falling p_T distribution, it is more likely for an outgoing particle to take a large fraction of the parent parton's momentum than for it to take a small fraction. Thus, single-particle triggers are biased towards large values of z. Now the fragmentation functions behave as powers of $1-z$ as z goes to one. As shown in Eqs. (5)–(7), these powers are 1–2 for mesons and 2–3 for baryons. Therefore, the trigger bias present in single-arm triggers causes a larger suppression for baryon production than for meson production. This means that for baryon production a larger fraction of the cross section at any fixed p_T will be made up of other competing processes than is the case for meson production.

A clearer understanding of this pattern can be obtained by studying the predictions of the CIM for p and $\bar{p}$ production in pp interactions.[22,24] Here, there are a variety of subprocesses, each of which is characterized by a scaling p_T^{-12} behavior. For proton production there are large contributions from "direct" production of protons as well as from diagrams which are proportional to valence quark distributions. However, for $\bar{p}$ production there is no direct term and the remaining CIM diagrams are proportional to small parton distributions such as the sea term. Therefore, one is led to the conclusion that there should be a large CIM contribution to proton production which could dominate over the lowest-order prediction. However, for $\bar{p}$ production the CIM terms are smaller and the lowest-order predictions should become dominant at a moderate value of p_T. This behavior can be verified by studying the scaling properties for p and $\bar{p}$ production. It has been observed[53] that p ($\bar{p}$) production scales as p_T^{-12} (p_T^{-8}) at fixed x_T and θ, in the region $p_T \lesssim 6$ GeV/c and $\sqrt{s} \lesssim 27.4$ GeV. The CIM prediction is p_T^{-12} in each instance, whereas the lowest-order subprocesses scale as p_T^{-4}. In actual practice, the scaling violations cause the lowest-order predictions to have a characteristic p_T power of about 6.5. The CIM prediction for proton production agrees with the data, but this is not the case for $\bar{p}$ production. Apparently, for $\bar{p}$ production the effects of the lowest-order terms are causing the p_T power to drop from 12 to about 8, a value which is intermediate between the predictions of the two types of subprocesses.

The observation of a p_T^{-12} behavior for proton

production is a crucial one, for the following reasons. For meson production the predictions for the p_T power were not too different between the CIM (p_T^{-8}) and the lowest-order $2 \to 2$ subprocesses modified by scaling violations ($p_T^{-6.5}$). In particular, parton k_T smearing, assumed to be coming in part from higher-order diagrams, can give rise to a p_T^{-8} behavior over a limited range of p_T.[4,5,7] However, for proton production the lowest-order subprocesses still predict a p_T exponent of about 6.5. In Fig. 13 the invariant cross-section predictions weighted by p_T^8 have been plotted at fixed x_T and θ. The characteristic rise with p_T is seen here, just as in the meson case.[4,5,7] There is no way that a behavior of p_T^{-12} can be obtained from these subprocesses. Therefore, in this particular reaction the trigger bias effect has resulted in a relative enhancement of the predictions of the CIM diagrams over those of the lowest-order diagrams, and this enhancement is made particularly evident by studying the p_T dependence at fixed x_T and θ.

Thus far, the baryon predictions have all been made for $\theta = 90°$. However, additional information may be obtained by studying, for example, the dependence on θ for fixed p_T. Alternatively, one can study the x_F dependence at fixed p_T. In either case, the behavior predicted by the lowest-order QCD subprocesses will be qualitatively the same as for the meson case,[3,5] since only the fragmentation functions have been changed. Therefore, the cross section will be roughly constant for $45° \lesssim \theta \leq 90°$ followed by a sharp falloff at smaller angles. This falloff occurs at a somewhat larger angle for baryons than for mesons due to the steeper fragmentation functions. This prediction is in agreement with the observed behavior for $\bar{p}$ production for $\sqrt{s} \geq 23$ GeV (Ref. 54) in pp collisions. However, for proton production a much flatter θ distribution is observed as a result of the leading-particle effect. At high p_T values the distribution does exhibit a decrease at small angles, but it is less drastic than for $\bar{p}$ or meson production.

This discrepancy for proton production is not unexpected and is, in fact, just another indication of the importance of the higher-order contributions. This latter category includes the "direct" terms of the CIM in which the observed proton comes directly from either the beam or target. It is interesting to note that these direct terms could be studied in detail by comparing the beam and target fragmentation regions for high-p_T proton production in πp interactions.

The above discussion shows that the θ dependence at fixed p_T supports the conclusion that there are higher-order types of diagrams which can make significant contributions to the observed baryon yields. For pp interactions these terms are largest for proton production, smallest for meson production, and of intermediate importance for $\bar{p}$ production.

V. SUMMARY AND CONCLUSION

The major goal of this analysis was to obtain predictions for baryon production from the lowest-order $2 \to 2$ subprocesses. In order to accomplish this, baryon fragmentation functions were required. Using new electroproduction data for p and $\bar{p}$ production, parametrizations of the required functions were obtained. In the process, a set of meson fragmentation functions was also obtained which reflected the effects of resonance decays. Using these improved fragmentation functions, predictions for both meson and baryon production were made. These predictions were based on the lowest-order $2 \to 2$ subprocesses modified by the QCD predicted scaling violations and parton k_T smearing. In calculating the latter effect, only the intrinsic parton k_T component was retained. This was estimated to correspond to $\langle k_T \rangle = 660$ MeV/c (using a Gaussian distribution) on the basis of dimuon production data. The reduced amount of k_T smearing means that the results are insensitive to off-shell kinematics, mass parameters, or k_T cutoffs. With these restrictions, no effects from higher-order diagrams are included other than the logarithmic Q^2 dependences of the coupling $\alpha_s(Q^2)$ and the parton distribution and fragmentation functions.

As expected, it was found that for moderate p_T values, e.g., 3 GeV/c, the theoretical predictions were below the data, thus indicating the presence of higher-order terms such as $2 \to 3$ subprocesses, CIM diagrams, etc. It was further found that the discrepancies between the lowest-order predictions and the data become greater in going from meson (~ 3) to $\bar{p}$ (~ 8) to p (~ 20) production. This pattern can be understood as being due to two competing effects. First, any subprocess in which the observed hadron is a fragment of an outgoing parton will suffer from trigger bias. This suppresses the lowest-order baryon predictions more than those for meson production. Second, the CIM diagrams for $\bar{p}$ production are not too large, being proportional to small parton densities such as the sea terms. Therefore, in the intermediate-p_T region the ratio of CIM to lowest-order terms is largest for p production, smallest for meson production, and intermediate for the $\bar{p}$ case. This pattern is also evident in the observed p_T dependences at fixed x_T and θ.

It is expected that at sufficiently large p_T the predictions of the lowest-order subprocesses should become dominant. Indeed, there is evi-

dence that for meson production this is the case for $\sqrt{s} \gtrsim 50$ GeV and $p_T \gtrsim 5$ GeV/c. On the other hand, this transition is expected to occur at a somewhat larger p_T value for $\bar{p}$ production and at an even larger value for p production. As these transitions occur one should observe a change in the p_T dependence at fixed x_T and θ. The p and $\bar{p}$ p_T powers should drop from 12 to about 6.5. Clearly, high-p_T ($p_T \gtrsim 10$ GeV/c) high-energy ($\sqrt{s} \gtrsim 50$ GeV) data with particle identification would be desirable in order to verify these predictions.

The results obtained here support the point of view that the description of high-p_T hadron production becomes less complicated as increasingly-larger-p_T regions are explored. The point at which the simplest, i.e., lowest-order, terms begin to dominate depends strongly, however, on both the particular beam/target combination[24] as well as the produced particle species. Thus, the description of single-particle p_T distributions using only the lowest-order $2 \to 2$ subprocesses does not constitute a test of QCD as such. Rather, it serves as a consistency check on the perturbation techniques used to obtain predictions from QCD. As one progresses from the high-p_T to the moderate-p_T range, contributions from higher-order terms and new types of subprocesses begin to be important. Sorting out these different contributions requires more information than is available from single-particle spectra. One must extend the analyses to include two-particle correlation studies, for example.[5] An interesting exercise along these lines would be to study the effects of final states with three high-p_T jets.[56,57] Such an extension of the basic perturbative QCD calculation would allow a further refinement of the estimates of the role played by more complex subprocesses such as those found in the CIM diagrams.

ACKNOWLEDGMENT

The author wishes to acknowledge useful discussions with S. J. Brodsky, D. Jones, R. D. Field, and E. Reya. This work was supported in part by the U.S. Department of Energy.

[1]B. L. Combridge, J. Kripfganz, and J. Ranft, Phys. Lett. 70B, 234 (1977).
[2]R. Cutler and D. Sivers, Phys. Rev. D 17, 196 (1978).
[3]J. F. Owens, E. Reya, and M. Glück, Phys. Rev. D 18, 1501 (1978).
[4]R. D. Field, Phys. Rev. Lett. 40, 997 (1978).
[5]R. P. Feynman, R. D. Field, and G. C. Fox, Phys. Rev. D 18, 3320 (1978).
[6]A. P. Contogouris, R. Gaskell, and S. Papadopoulos, Phys. Rev. D 17, 2314 (1978).
[7]J. F. Owens and J. D. Kimel, Phys. Rev. D 18, 3313 (1978).
[8]D. Gross and F. Wilczek, Phys. Rev. Lett. 26, 1343 (1973).
[9]H. D. Politzer, Phys. Rev. Lett. 26, 1346 (1973).
[10]D. Amati, R. Petronzio, and G. Veneziano, Nucl. Phys. B140, 54 (1978); B146, 29 (1978).
[11]See also Ref. 12 and references contained therein.
[12]H. D. Politzer, talk presented at the 1978 International Conference on High Energy Physics, Tokyo, Caltech Report No. CALT-68-682, 1978 (unpublished).
[13]A. De Rújula, H. Georgi, and H. D. Politzer, Ann. Phys. (N.Y.) 103, 315 (1977).
[14]M. Glück and E. Reya, Phys. Rev. D 14, 3034 (1976).
[15]J. F. Owens, Phys. Lett. 76B, 85 (1978).
[16]T. Uematsu, Phys. Lett. 79B, 97 (1978).
[17]M. Della Negra *et al.*, Nucl. Phys. B127, 1 (1977).
[18]A good review of parton-k_T smearing in high-p_T calculations can be found in Ref. 19.
[19]R. D. Field, talk presented at the 1978 Marseille meeting on Hadron Physics at High Energies, Caltech Report No. CALT-68-672, 1978 (unpublished).
[20]C. Sachrajda, Phys. Lett. 76B, 100 (1978).
[21]W. E. Caswell, R. R. Horgan, and S. J. Brodsky, Phys. Rev. D 18, 2415 (1978); R. R. Horgan and P. N. Scharbach, Phys. Lett. 81B, 215 (1979).
[22]R. Blankenbecler, S. J. Brodsky, and J. F. Gunion, Phys. Rev. D 18, 900 (1978).
[23]Reference 22 contains a detailed discussion of the normalization and scaling behavior of the various CIM subprocesses. These ideas are compared with the data in Ref. 24.
[24]D. Jones and J. F. Gunion, Phys. Rev. D 19, 867 (1979).
[25]S. D. Drell and T. M. Yan, Phys. Rev. Lett. 25, 316 (1970); Ann. Phys. (N.Y.) 66, 578 (1971).
[26]G. Altarelli, G. Parisi, and R. Petronzio, Phys. Lett. 76B, 351 (1978); 76B, 356 (1978).
[27]F. Halzen and D. M. Scott, Phys. Rev. Lett. 40, 1117 (1978).
[28]Reviews of lepton pair production may be found in Refs. 29 and 30.
[29]R. C. Hwa, Review talk given at the IXth International Symposium on High Energy Multiparticle Dynamics, Tabor, Czechoslovakia, Univ. of Oregon Report No. OITS 95, 1978 (unpublished).
[30]E. L. Berger, in *New Results in High Energy Physics—1978*, proceedings of the 3rd International Conference at Vanderbilt University, edited by R. S. Panvini and S. E. Csorna (AIP, New York, 1978).
[31]C. Sachrajda, Phys. Lett. 73B, 185 (1978).
[32]D. Kaplan *et al.*, Phys. Rev. Lett. 40, 435 (1978).
[33]J. F. Owens, Phys. Rev. D 18, 2462 (1978).
[34]M. Glück and E. Reya, Nucl. Phys. B145, 24 (1978).
[35]R. D. Field and R. P. Feynman, Nucl. Phys. B136, 1 (1978).
[36]J. F. Martin *et al.*, Phys. Rev. D (to be published).
[37]B. Andersson, G. Gustafson, and C. Peterson, Nucl.

Phys. B135, 273 (1978).
[38]E. M. Ilgenfritz, J. Kripfganz, and A. Schiller, Acta Phys. Pol. B9, 881 (1978).
[39]R. D. Field and R. P. Feynman, Phys. Rev. D 15, 2590 (1978).
[40]The isospin sum rule is slightly violated when the effects of the baryon sector are included. This is due to the fact that to correctly satisfy the sum rule the primary baryon fragmentation functions should be used, instead of Eq. (7). This is, however, a small effect proportional to $1-P$.
[41]Ch. Berger *et al.*, Phys. Lett. 70B, 471 (1977).
[42]B. P. Roe, in *Proceedings of the 1975 International Symposium on Lepton and Photon Interactions at High Energies, Stanford, California*, edited by W. T. Kirk (SLAC, Stanford, 1976), p. 551.
[43]M. Derrick *et al.*, Phys. Rev. D 17, 1 (1978).
[44]Additional neutrino data have been obtained from Ref. 39.
[45]J. Bell *et al.*, Phys. Rev. D 19, 1 (1979).
[46]J. P. Berge *et al.*, Phys. Rev. D 18, 3905 (1978).
[47]R. Brandelik *et al.*, Phys. Lett. 67B, 358 (1978).
[48]D. Antreasyan *et al.*, Phys. Rev. Lett. 38, 112 (1978).
[49]F. W. Büsser *et al.*, Nucl. Phys. B106, 1 (1976).
[50]G. Kourkoumelis *et al.*, paper submitted to the Tokyo High Energy Physics Conference, 1978 (unpublished); L. K. Resvanis (private communication).
[51]A. G. Clark *et al.*, Phys. Lett. 74B, 267 (1978).
[52]B. G. Pope, in *Particles and Fields—1977*, proceedings of the Meeting of the APS Division of Particles and Fields, Argonne, Illinois, edited by P. A. Schreiner, G. H. Thomas, and A. B. Wicklund (AIP, New York, 1978), p. 239.
[53]D. Antreasyan *et al.*, Phys. Rev. Lett. 38, 115 (1977).
[54]B. Alper *et al.*, Nucl. Phys. B87, 19 (1975).
[55]The $\bar{p}$ data from Ref. 54 have been renormalized by a factor of 0.5 so as to agree with the results of Ref. 53 in the kinematic region where the data sets overlap.
[56]B. L. Combridge, Phys. Rev. D 18, 734 (1978).
[57]J. Kripfganz and A. Schiller, Phys. Lett. 79B, 317 (1978).